5-4-2016

Prediction, Minimization and Propagation of Sonic Boom from Supersonic Bodies

Jeffrey Krampf
Washington University in St. Louis

Junhui Li
Washington University in St. Louis

Ramesh K. Agarwal
Washington University in St. Louis

MEMS 500: Independent Study

Prediction, Minimization and Propagation of Sonic Boom from Supersonic Bodies

Jeffrey Krampf

Research Advisor: Professor Ramesh K. Agarwal

Note: Attached paper describes some of the results of the independent study

Department of Mechanical Engineering & Materials Science
Washington University in St. Louis

Spring 2016

Prediction, Minimization and Propagation of Sonic Boom from Supersonic Bodies

Jeffrey Krampf, Junhui Li and Ramesh K. Agarwal

Department of Mechanical Engineering and Materials Science

Washington University in St. Louis, St. Louis, MO 63130

This paper first describes the numerical simulation and shape optimization of the Lockheed SEEB-ALR and 69 Degree Delta Wing-Body for computing the sonic boom signature in the nearfield and its minimization using a genetic algorithm. Then the propagation of sonic boom in the atmosphere is simulated all the way to the ground for both the original and optimized body shapes. For flow field calculation, the commercial CFD flow solver ANSYS Fluent is employed. The near field pressure disturbance is used to determine the strength of the sonic boom signature. The computational results for the two cases are compared with the experimental data. The body shapes are then optimized using a single-objective genetic algorithm. The results show a significant decrease in strength of the sonic boom. The pressure data from these two models is then scaled and propagated through the atmosphere using the NASA Langley Research Center sBOOM code to predict the far field signature of these bodies at the scale of a commercial supersonic aircraft.

I. Introduction

Supersonic aircraft flow fields and their sonic boom minimization have been widely studied in recent years. Because of the limitation of physical testing, CFD technology provides an attractive alternative to aid in the design of aerospace vehicles. Today, improvements in Reynolds-averaged Navier-Stokes (RANS) computations can be attributed to an increase in computational power, which allows for treatment of more complex geometries with larger meshes, better numerical algorithms and improved turbulence models to reduce the predictive error. As computational power continues to increase, numerical optimization techniques are being combined with CFD to further aid in the design process.

In this paper, two cases from the recent AIAA Sonic Boom Prediction Workshop[1] have been simulated and optimized to reduce the sonic boom signature. The AIAA Sonic Boom Prediction Workshop presented three models for the study of predicting sonic boom signatures and sonic boom propagation. In this paper, the Lockheed SEEB-ALR and 69 Degree Delta Wing-Body are considered. The grid generation is conducted by ANSYS ICEM. Flow calculations are performed with ANSYS Fluent using the compressible Euler equations. Excellent agreement between the computed pressure distributions and experimental results at all positions of the models is obtained. Shape optimization of the bodies to minimize the sonic boom signature is then performed using a genetic algorithm (GA). The optimized shapes show a decrease in the strength of the sonic boom signature.

Propagation of the modeled pressure data to ground level is performed using sBOOM software available from the NASA Langley Research Center[2]. The sBOOM program utilizes the augmented Burgers equation to propagate pressure data from a defined cruise altitude to a prescribed distance from the body. In this paper, a cruise altitude of 45,000 ft is used, and the pressure signature is propagated down to ground level. In order for the pressure disturbance from the small wind tunnel scale models to be significant enough to propagate to ground level from this cruise altitude, they are scaled up to the size of larger commercial craft for the calculation. The scaling and propagation are both done internally in sBOOM where the signal is propagated to the smaller scaled distance and the ray tubes are then scaled up to the larger scale of "actual" aircraft size. A full-size length of both the models used in this paper was approximately 202 ft based on the Concord supersonic aircraft.

II. Test Cases

A.SEEB-ALR

Lockheed SEEB-ALR is an axisymmetric wind tunnel model shown in Figure1. The reference length of the model is 17.68 inches [3]. The model is placed in wind tunnel at free stream Mach number of 1.6 at an angle of attack of 0 degree. The Reynolds number based on freestream velocity is $\mathrm{Re} = 6.42 \times 10^6$.

The grid is generated by ICEM CFD and contains 1.4 million hexahedra cells as shown in Figure 2. The model is split in half by considering symmetry in order to reduce the computational effort. The mesh is aligned with the shock wave at Mach angle of 38.68 degrees in the radial direction. According to the geometry from AIAA Sonic Boom Workshop, the front cusp is a small plane which allows hexahedra cells. The characteristic length of this plane of front cusp is less than 0.1% of the reference length of the model.

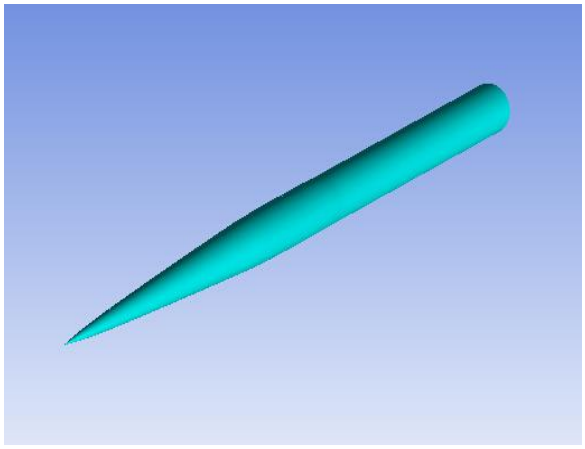

Fig. 1 SEEB-ALR geometry.

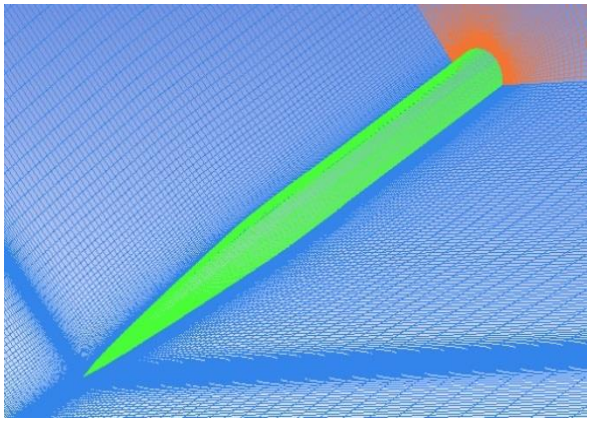

Fig. 2 Mesh around SEEB-ALR.

B.69 Degree Delta Wing-Body

The 69 Degree Delta Wing-Body is also a symmetric body shown in Figure 3 and Figure 4. The Wing-Body model and support structure are both included in the simulation. The reference length of the model is 6.9 inches. The model is placed in a wind tunnel with freestream Mach number of 1.7 at an angle of attack of 0 degree. The Reynolds number based on the freestream velocity is $\mathrm{Re} = 2.43 \times 10^6$.

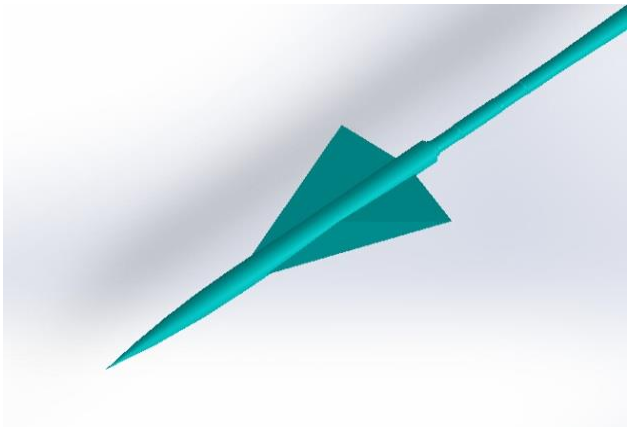

Fig. 3 Geometry of 69 Degree Delta Wing-Body.

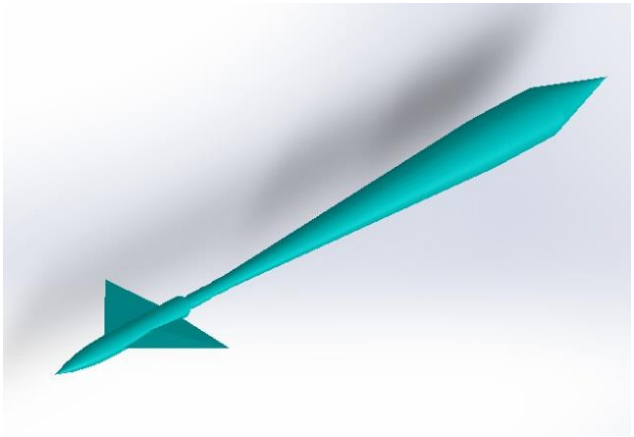

Fig. 4 Geometry of 69 Degree Delta Wing-Body with support structure.

The grid is generated by ICEM CFD and contains 4.57 million hexahedra cells as shown in Figure 5 and Figure 6. The model is again split in half and is solved as a symmetric model. Y-Blocks are applied to build the mesh near the delta wing. The mesh is aligned with the shock wave at Mach angle 36.03 degrees in the radial direction.

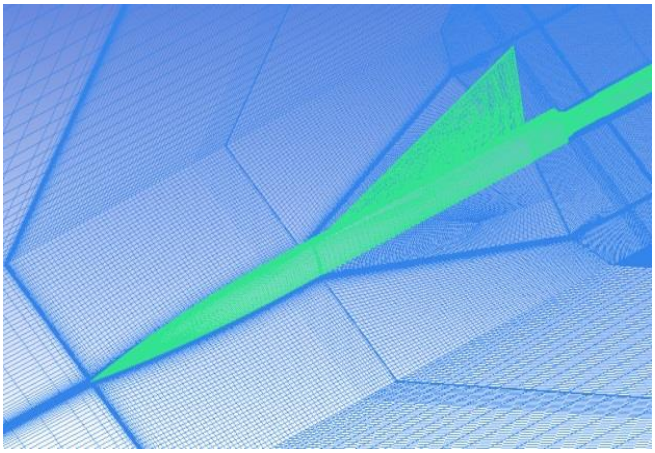

Fig. 5 Mesh around the 69 Degree Delta Wing-Body.

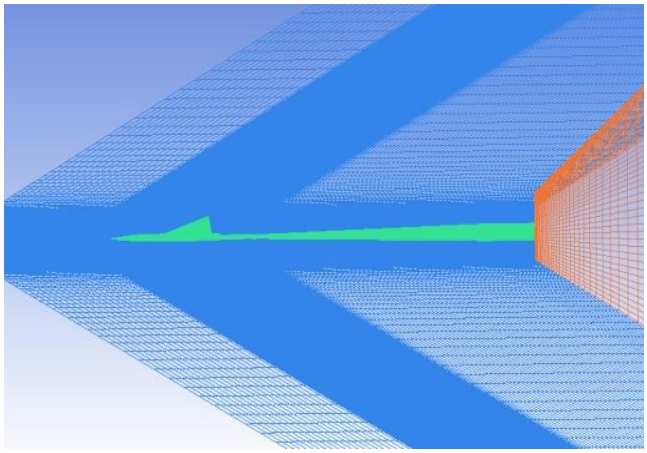

Fig. 6 Mesh around the 69 Degree Delta Wing-Body with support structure

III. Simulation Results

A.SEEB-ALR

The results of SEEB-ALR simulation are shown in Figures 7 and 8. As described in the AIAA Sonic Boom Workshop, ΔP/P (near field pressure disturbance) is defined to be the signature of the sonic boom which represents the strength of the shock wave. The pressure disturbances obtained from the simulation at a distance of 21inches and 31inches from the body are plotted against the experimental data. It can be seen that excellent agreement between the simulation and the experimental data is obtained. The simulations successfully predict the maximum disturbance at the same position with the same magnitude when compared to the experimental data. Thus, the SEEB-ALR simulation has been successfully verified and validated; this pressure disturbance is used as the baseline result to minimize its signature by changing the shape of the body using the single objective genetic algorithm.

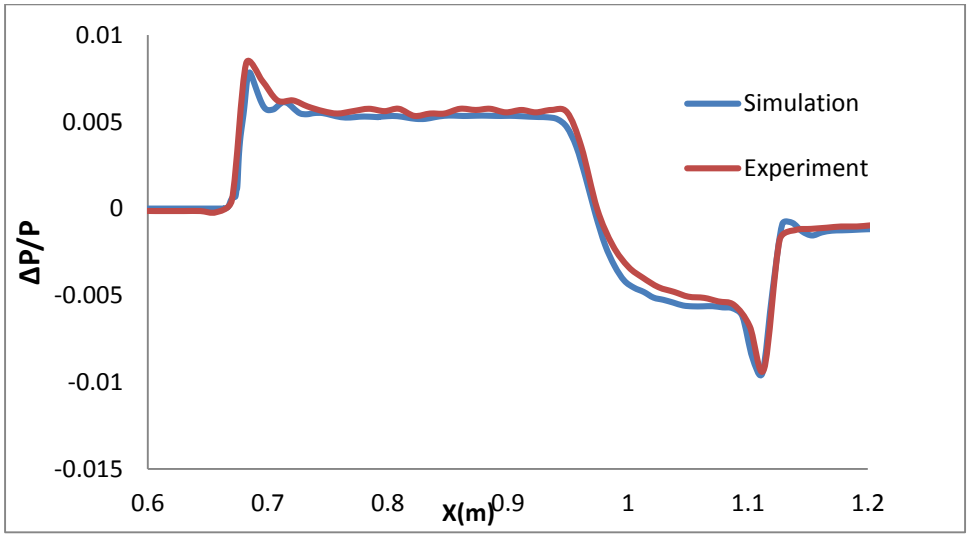

Fig. 7 Pressure disturbance along x-direction at H = 21in.

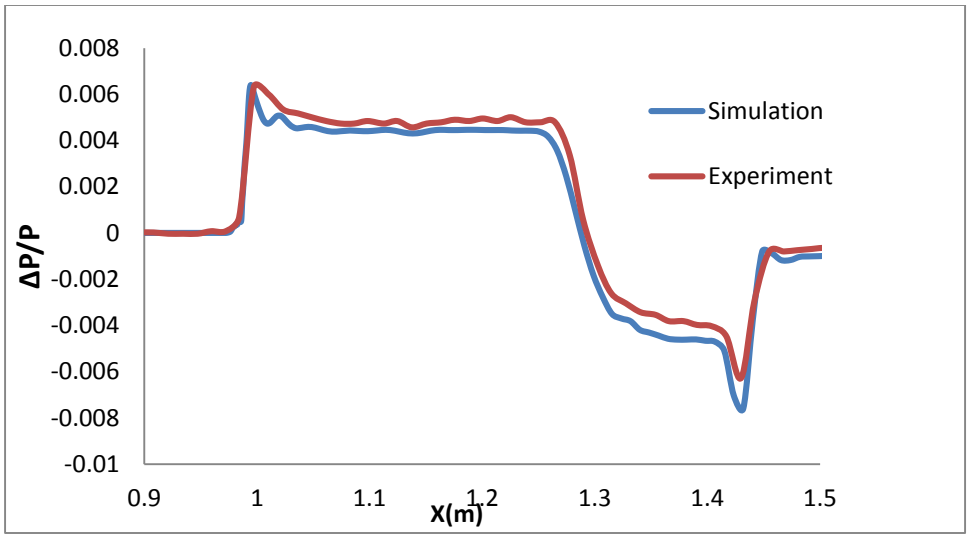

Fig. 8 Pressure disturbance along x-direction at H = 31in.

B. 69 Degree Delta Wing-Body

The results for 69 degree Delta Wing-Body are shown in Figures 9 and 10. Figures 9 and 10 present the ΔP/P along x-direction at 25 inches ($3.6L_{Ref}$) away from the body at different azimuthal angle φ. The simulation results show very good accuracy at $\varphi = 0^o$ and $\varphi = 90^o$. These results demonstrate that the Y-Block mesh provides enough quality near the delta wing for accurate computations. Thus, the Delta Wing-Body simulation has been successfully verified and validated; this pressure disturbance is then used as a baseline result to minimize its signature by changing the shape of the body using the single objective genetic algorithm.

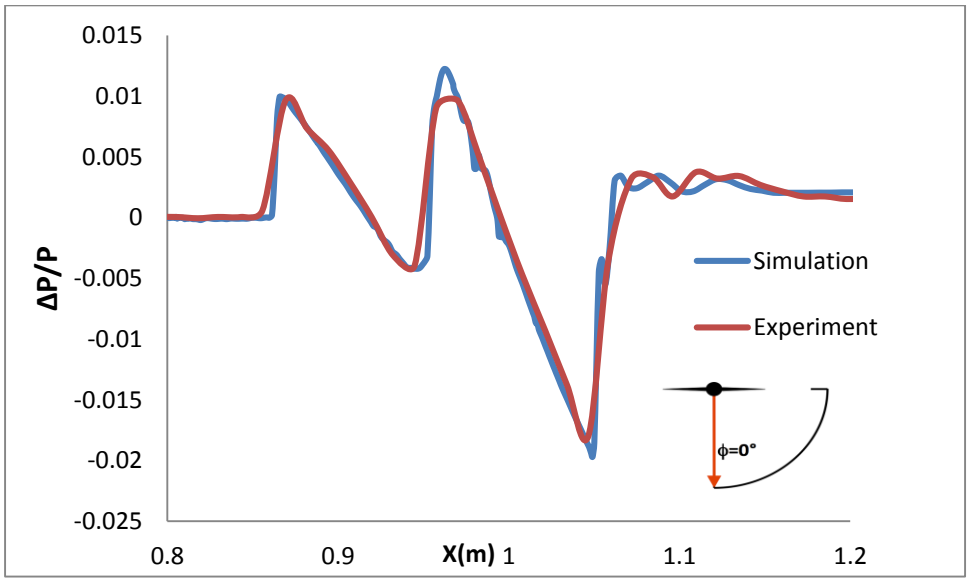

Fig. 9 Pressure disturbance along x direction at $\varphi = 0°$

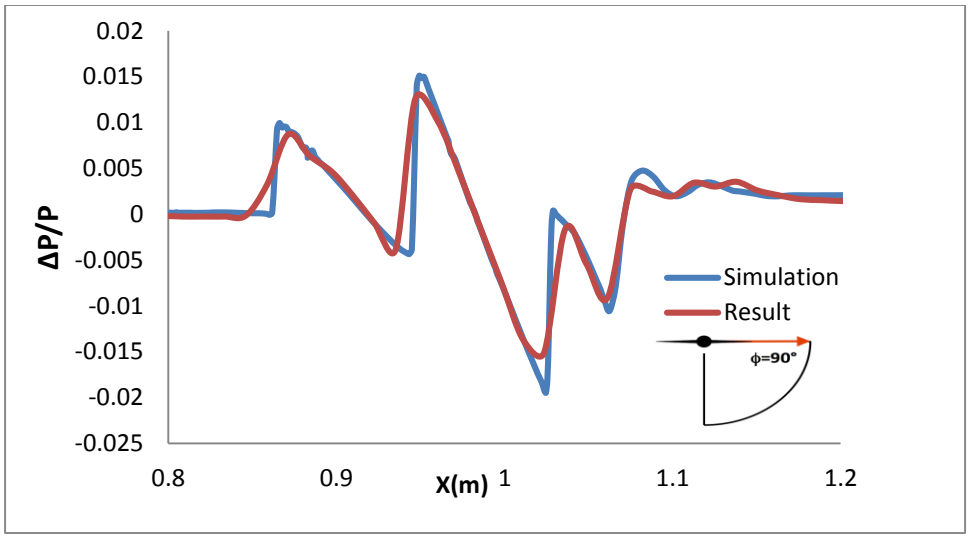

Fig. 10 Pressure disturbance along x direction at $\varphi = 90°$

IV. Genetic Algorithm

Genetic algorithms are a class of stochastic optimization algorithms inspired by biological evolution [4]. In GA, a set of input vectors, called *individuals*, is iterated over, successively combining traits of the best individuals until convergence is achieved [5]. In general, a GA employs the following steps:

1. *Initialization*: Randomly generate N individuals.
2. *Evaluation*: Evaluate the fitness of each individual.
3. *Natural Selection*: Remove a subset of the individuals (often individuals with the lowest fitness).
4. *Reproduction*: Create a new generation of individuals.
    a. *Parent Selection*: Select pairs of individuals to produce an offspring.
    b. *Crossover*: Exchange information between the parent individuals.
    c. *Mutation*: Randomly alter some small percentage of the population.
5. *Check for Convergence*: If the solution has converged, return the fittest individual. If the solution has not yet converged, repeat the cycle starting at step 2 with the new generation.

Multi-objective genetic algorithms (MOGAs) differ from single-objective genetic algorithm (SOGA) in that the fitness of individuals is not determined by a single objective or fitness function, but by two or more optimization objectives [6,7]. These objectives are sometimes in conflict [8]. Since only the strength of the shockwave will be minimized, a SOGA is used in the present work.

Figure 11 shows the general schematic of the shape optimization procedure. The four processes are: (1) Shape generation, (2) Meshing the Body shape, (3) Performing simulation, and (4) Optimization using SOGA.

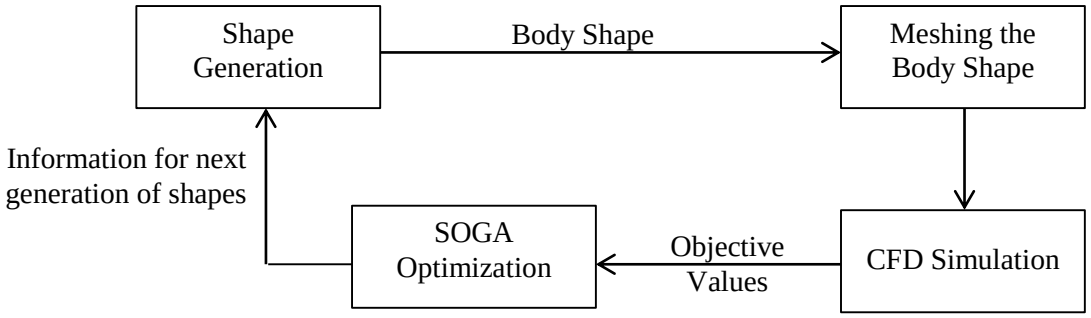

Fig. 11 General schematic of information flow in shape optimization process.

Bezier curve polynomials are used to create the body profile. A Bezier curve is a parametric curve that is defined by control points, whereas the curve itself generates a smooth path between the control points. They have favorable characteristics for use in a GA since the initial and final points and slopes can be fixed, control point information between individuals is easily swapped, and changing a control point results in a similar change to the curve itself [9]. Figure 12 shows an example of a set of three random curves in a generation. These curves represent the tip of the SEEB-ALR model. The green dots represent the control points, whereas the red line represents the resulting curve. Note that in all three cases, the first two and last two control points are fixed to ensure a blunt leading edge and appropriate size constraints on the shape. The shape is axisymmetric about the bottom x-axis and travels to the left at supersonic speeds.

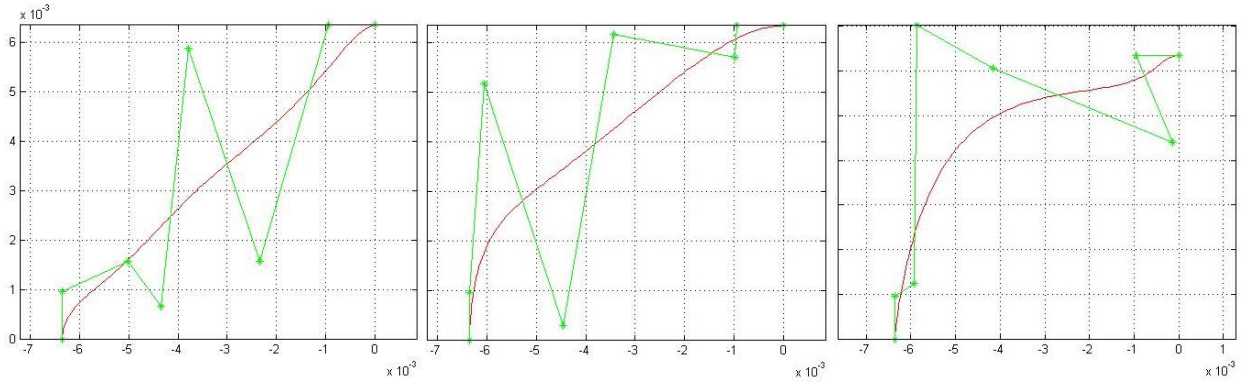

Fig. 12 Three randomly generated curves and their Bezier control points.

Similar random curves are generated for a typical generation of GA consisting of ten random shapes (individuals). The meshes around these random shapes are generated and the flow field is computed. Then the sonic boom signatures of random shapes are recorded and uploaded into the SOGA code, which conducts evaluation, natural selection, and reproduction functions on the data. During the optimization process, the objective function information for each body shape is always retained. The implementation of various steps in SOGA is described below:

(a) *Evaluation and Natural Selection*

The objective values of random shapes are analyzed and compared to each other. In the present case, minimization of objective value is desired. Each objective value is sorted from best to worst, where the lowest value is the best and highest value is the worst. The fittest half of the individuals "survive" and have a chance to reproduce and influence the next generation in SOGA.

(b) *Reproduction and Mutation*

Reproduction involves parent selection, crossover, and mutation. From the remaining data, pairs of parent shapes are selected using a skewed random draw; more fit a function is, higher is its probability of being selected. The paired curves then undergo crossover, where they exchange Bezier point information. The exchange can be a complete swap of certain points or a weighted average of the characteristics of certain points. Both type of crossover and the type of exchange are selected at random. This process is repeated until the desired number of daughter shapes is created and a new generation is formed. The final step is mutation. Randomly selected Bezier points of randomly selected curves are randomly altered, adding more diversity into the generation to increase the range of body shapes.

(c) *Solution Convergence*

Finally, the SOGA checks if the curves obtained in a given generation satisfy the convergence criteria. The convergence criteria are based on whether the body shapes in a generation are close to each other and the difference in the objective values in that generation is within a specified tolerance. If the change in the body shape and the objective values for a few subsequent generations (usually 2 to 3) are in acceptable range, the solution is considered converged. Once the solution converges, SOGA gives the fittest (almost optimal) body shape meeting the desired objective. If the solution has not yet converged, the new generation is loaded into the shape generating function in Fig. 11 and the process is repeated. Figure13 shows a detailed schematic of information flow in the optimization process.

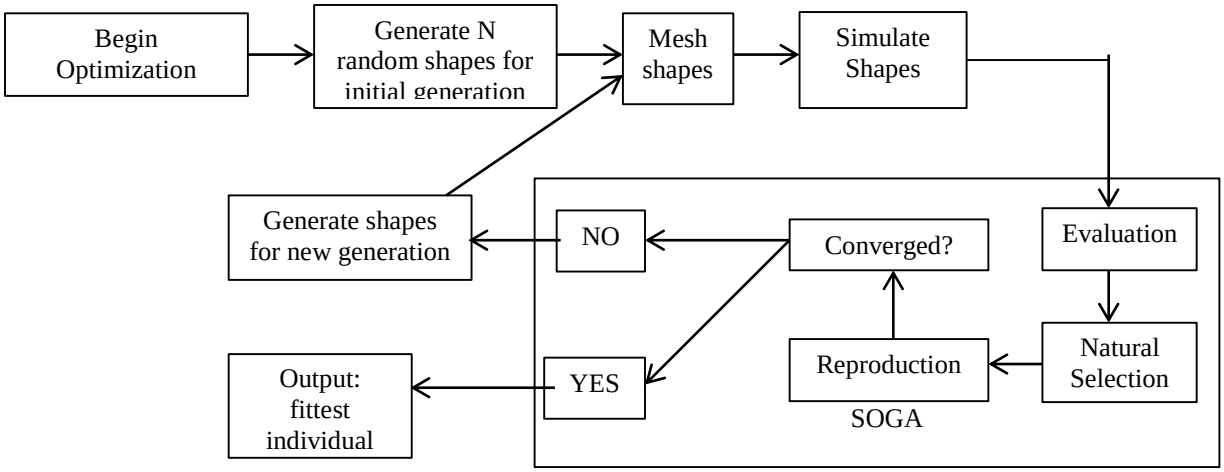

Fig. 13 Schematic of information flow in SOGA optimization process.

V. Sonic Boom Optimization Results

The optimization is performed in two steps by employing SOGA. During the first round of optimization, almost converged solution for minimized sonic boom is obtained which is further refined in second round of SOGA optimization.

A. First round of Genetic Algorithm optimization

The first round of Genetic Algorithm optimization is a coarse optimization. A large control point window is defined to allow enough diversity in random shapes. Table 1 shows the parameters used in first round of GA optimization. Each generation has 10 individuals.

Table 1: Genetic Algorithm parameters for first round of GA optimization

GA parameters	Description
Generation Size	10 individuals per generation
Number of Generations	Maximum of 100 generations if convergence not reached
Selection Type	Roulette Wheel Selection
Crossover Rate	0.5
Mutation Rate	0.4
Error of Mutation Constant	0.8, which determines how much mutation affects the curve as generations proceeds

The front part of fuselage is generated by rotating one Bezier curve. Six control points are set to be the constraints on the random curves. To ensure the starting point and ending point of the curve to be fixed, the 1st and 6th control point are fixed. To ensure the smooth transition from cone to cylinder, the 5th control point is also fixed. The 5th control point and 6th control point define the slope of Bezier curve at the end to be 0. There are 3 control points that are varied randomly in each shape. For each control point, a window which constrains the possible region of a control point is defined. The upper limit and lower limit of the all the six control point is presented in Table 2.

Table 2: Coordinate range for each control point of the Bezier curve in first round of GA optimization

Coordinate	Upper limit	Lower limit
x_1	Fixed at x=0	
x_2	0	5
x_3	5	10
x_4	10	16.5
x_5	Fixed at x=16.5	
x_6	Fixed at x=17.692413	
y_1	Fixed at y=0.005	
y_2	0	0.5
y_3	0	0.6
y_4	0	0.8
y_5	Fixed at y=0.69764638	
y_6	Fixed at y=0.69764638	

The first round of Genetic Algorithm optimization is completed by 19 generations. The objective functions are defined as $Max|P - Pinf| = Max|P - 101325|$. We avoid dividing this number by reference pressure in order not to make very small. Figure 14 shows the convergence process for minimization of fitness value ($Max|P - Pinf|$) as the generations incresae. The fitness value gradually decreases from 817Pa to 572Pa.

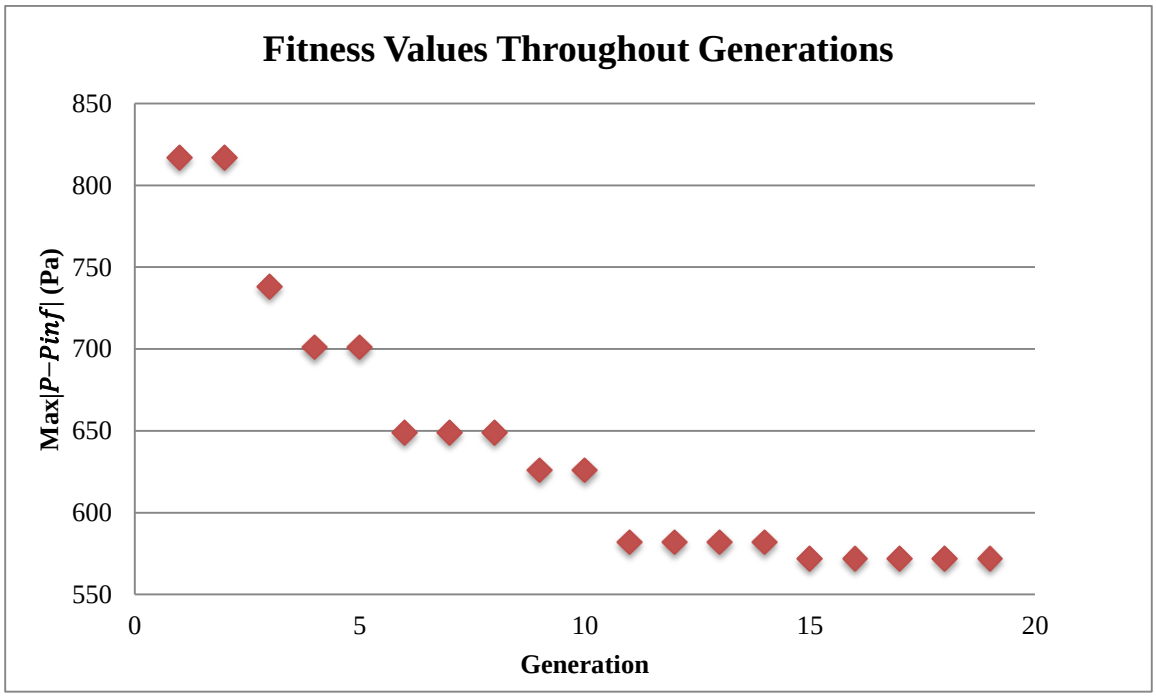

Figure 14: Fitness Value $|P - Pinf|$ in various generations of GA in 1st round in GA optimization

We choose the best shape in Generation 2, Generation 5, Generation 10 and Generation 19 (the final shape of first round of GA) to explore how the shape change affects the fitness value $|P - Pinf|$. The comparison are presented in Figure 15 which shows that the optimized shape in first round GA optimization does show larger difference from the original shape. The best shape in 19th generation, as the final best shape of in this first round, is much smoother than the original shape.

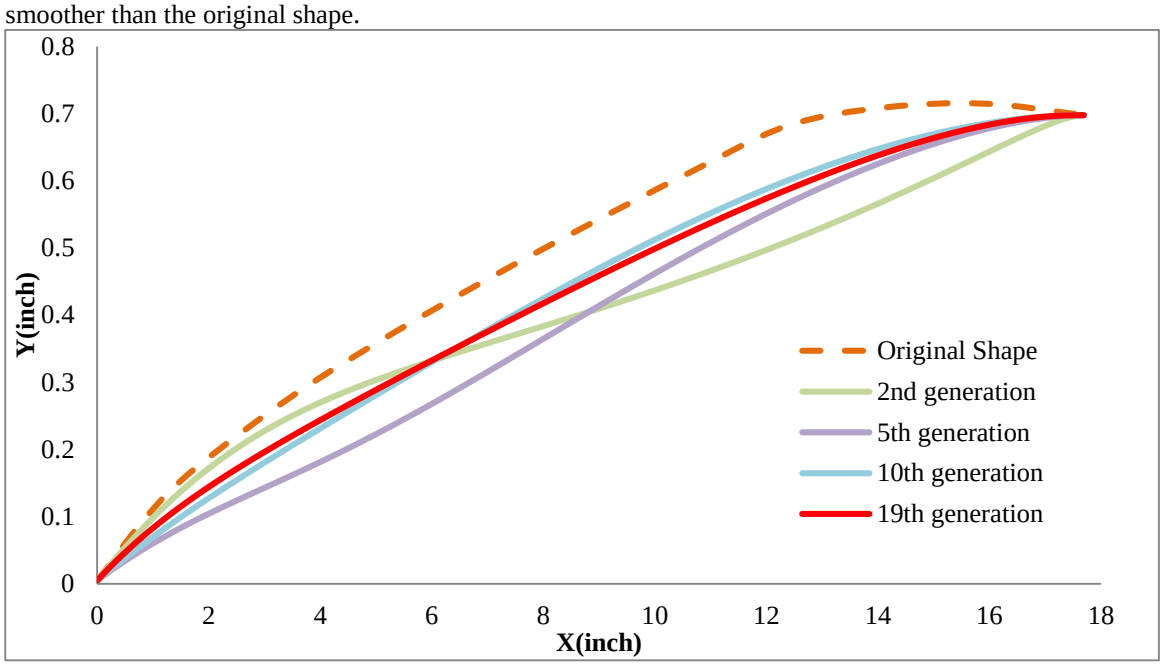

Figure 15: The change in body shape in different generations of GA optimization

The comparison of boom signature from original SEEB-ALR and the optimized shape in the first round of GA is presented in Figure 16. The pressure disturbance is smaller in magnitude for the optimized shape compared to the original SEEB-ALR model.

For the original SEEB-ALR, the maximum $|P - Pinf|$ occurs at x=0.69m and x=1.1m. At these locations, the strength of shock wave is reduced significantly. The expansion wave region is originally from 0.93m to 1.07m; this region becomes larger from 0.85m to 1.1m for the optimized model.

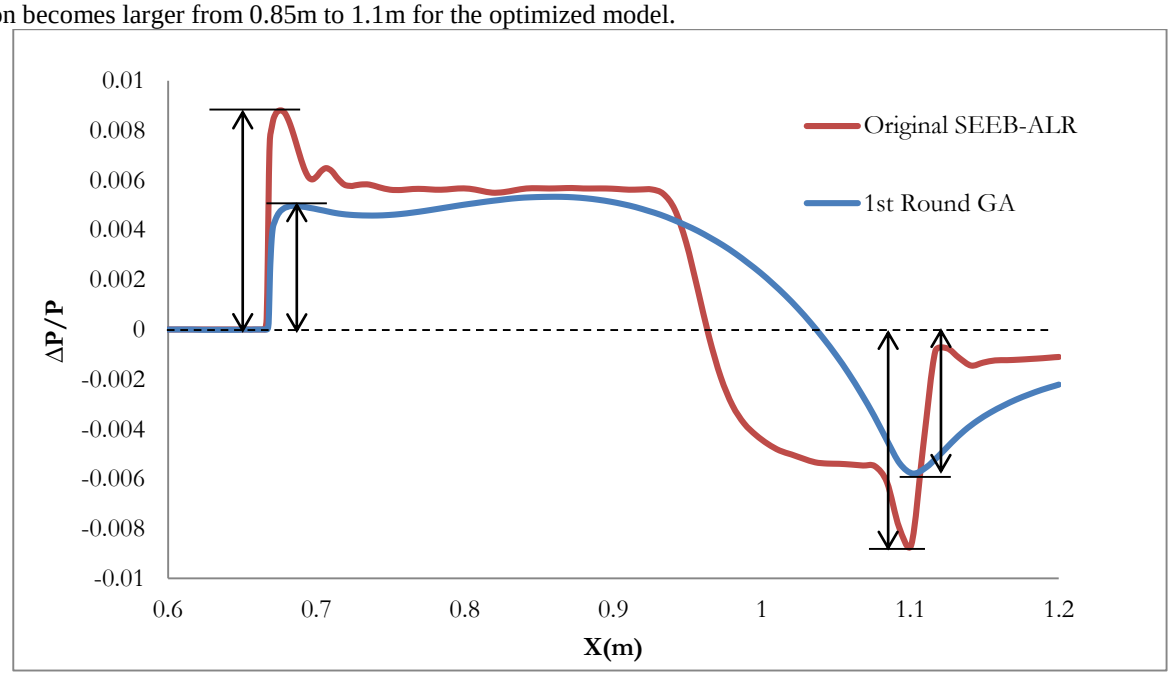

Figure 16: The comparison of pressure disturbance along x-direction between the optimized shape from 1st round of GA optimization and the original SEEB-ALR shape

Table 3 shows the reduction in sonic boom signature in 1st round of Genetic Algorithm optimization. Compared to the maximum pressure disturbance of the original SEEB-ALR, the optimized shape from 1st round of GA optimization minimized its value by 35.8%. Thus the sonic boom signature is significantly minimized. The maximum strength of shock wave becomes much weaker, which will reduce the ground noise. This result is further optimized in the second round of Genetic Algorithm optimization.

Table 3: Optimization result of first found Genetic Algorithm optimization

	Original SEEB-ALR	1st Round GA Optimized Shape
$Max\|P - Pinf\|$	892Pa	572Pa
$Max\left\|\frac{\Delta P}{P}\right\|$	0.008803	0.005645
Improvement	35.8%	

B. Second round of Genetic Algorithm

The second round of GA is based on the best shape obtained from the first round of GA. The window of each control point in the first round of GA was fairly large, which ensured wide range of random positions for all control points. The large window reduced the possibility of the best shape to be achieved. Hence, in second round of GA, the window of each control point is set to be a small region around the control point positions of best shape from the first round of GA optimization. Table 4 shows the control point window for second round of GA optimization.

Table 4: Coordinate range for each control point of the Bezier Curve of Second round of GA optimization

Coordinate	Upper limit	Lower limit
x_1	Fixed at x=0	
x_2	2.5	3.5
x_3	6	7
x_4	10	12.5
x_5	Fixed at x=16.5	
x_6	Fixed at x=17.692413	
y_1	Fixed at y=0.005	
y_2	0.25	0.35
y_3	0.25	0.35
y_4	0.6	0.7
y_5	Fixed at y=0.69764638	
y_6	Fixed at y=0.69764638	

Table 5 provides the parameters setting for second round of GA optimization. For this round, the objective is to further refine the optimal shape obtained from first round and thus further reduce the boom signature.The GA parameters are redefined to achieve this goal. Since the window of each control point is much smaller this time, to many individuals are not needed in a given generation. Thus, the number individual members per generation is reduced to make the generation grow faster and the mutation rate is added to have more diversity in offsprings from the parent generation. With these settings, quick convergence with a better fitness value is expected in this round of GA optimization.

Table 5: Genetic Algorithm parameters for second round of GA optimization

GA parameters	Description
Generation Size	6 individuals per generation
Number of Generations	Maximum of 50 generations if convergence not reached
Selection Type	Roulette Wheel Selection
Crossover Rate	0.5
Mutation Rate	0.6
Error of Mutation Constant	0.8, which determines how much mutation affects the curve as generations proceeds

The second round of Genetic Algorithm optimization is completed by 11th generation. The objective functions are again defined as $Max|P - Pinf| = Max|P - 101325|$. Figure 17 shows the variations of fitness value $Max|P - Pinf|$ with the advancing generations. This time the fitness value quickly converges to 548Pa in only 5 generations. After that the best fitness value remains the same for six additional generations which proves that the best shape now should be the optimal result of the optimization.

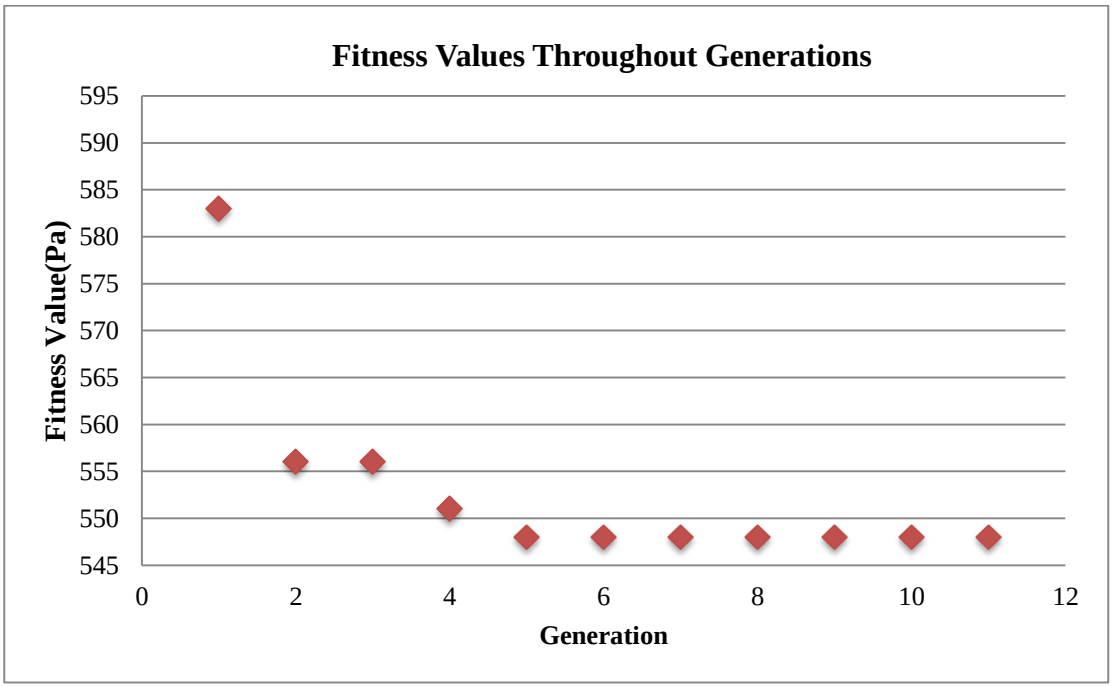

Figure 17: Fitness Value $|P - Pinf|$ in various generations of GA in 2nd round of GA optimization

Figure 18 shows the best shape and its control points in the 2nd round of GA optimization. Figure 19 shows the comparison of the best shapes from 1st and 2nd round of GA optimization with the SEEB-ALR original shape. Compared to the 1st round optimization shape, the best shape from 2nd round optimization has some additional improvements in the smoothness of the shape.

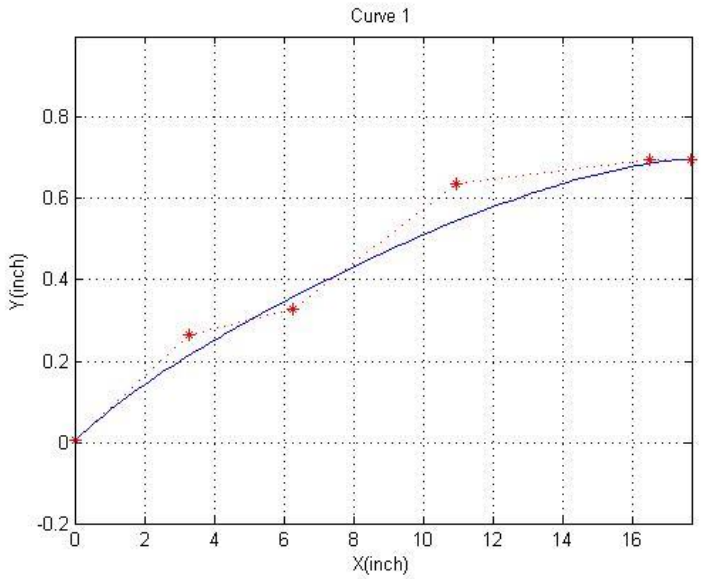

Figure 18: The optimal shape and its control points from 2nd round of GA optimization

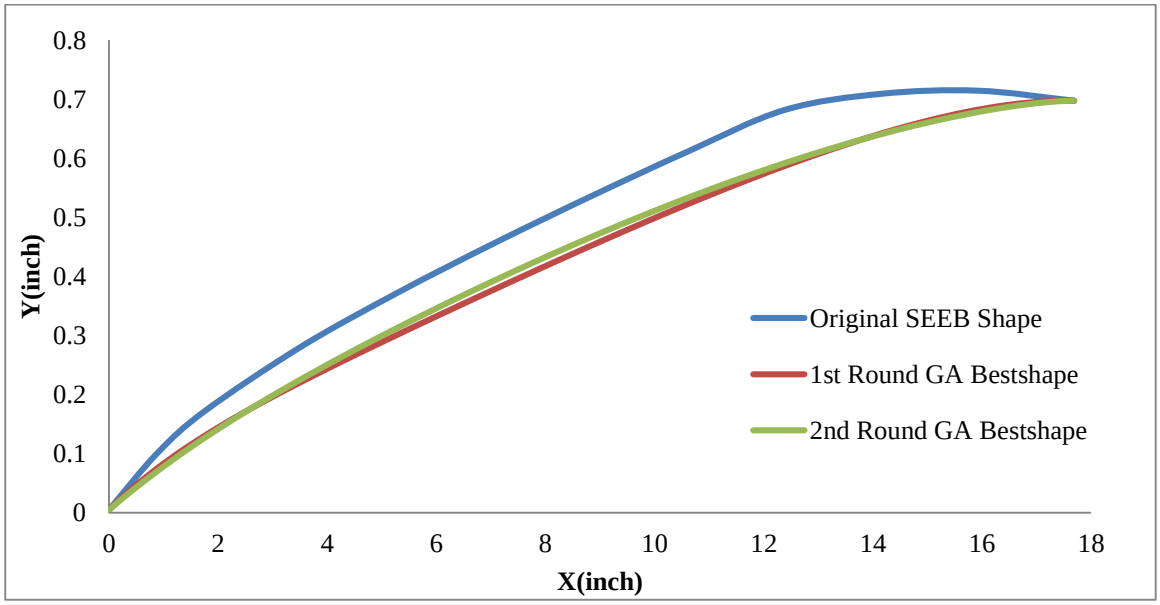

Figure 19: Comparison of optimized shapes from 1st round and 2nd round of GA optimization

Figure 20 provides the distribution of Pressure Disturbance along x-direction. The result from 2nd round of GA optimization is compared with the result from 1st round of GA optimization and the original SEEB-ALR. Though the maximum value of $|P - Pinf|$ does not have huge improvement, the tendency of the pressure distribution from 2nd round of GA shows some difference compared to that from 1st round of GA. The region of expansion wave is continuously extended. Based on this pressure distribution, a shock wave is generated which is followed by a large region of the expansion wave.

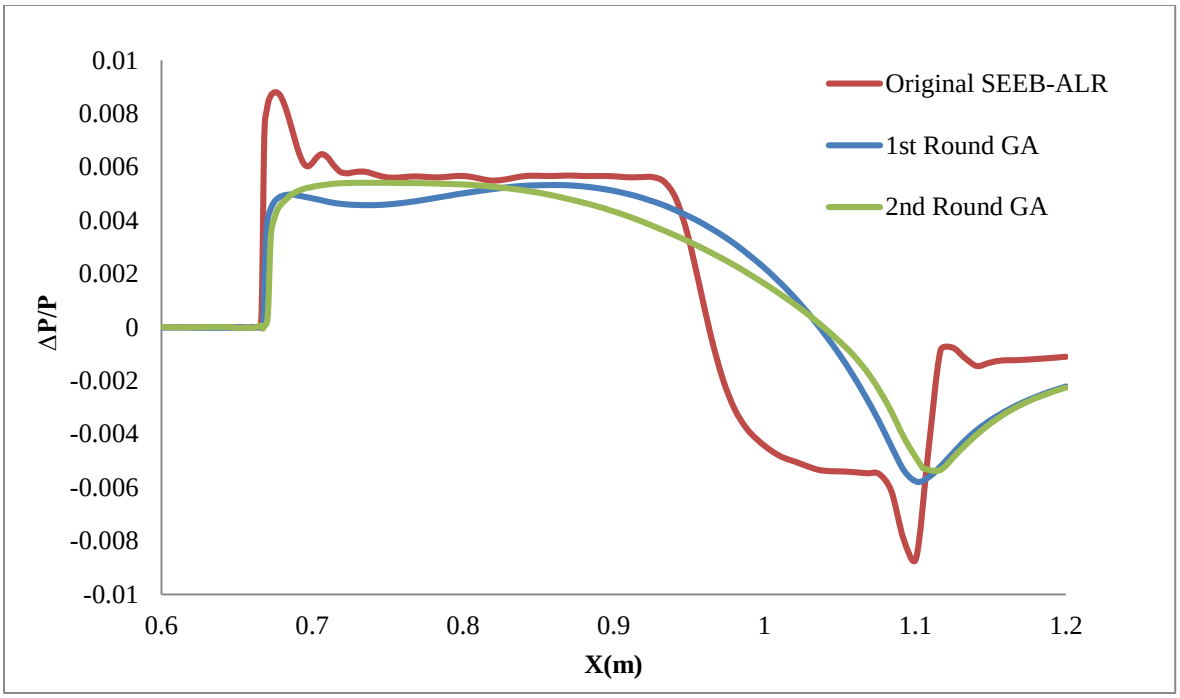

Figure 20: Comparison of pressure disturbance among optimized shape from 1st round of GA optimization, 2nd round of GA optimization, and original SEEB-ALR shape along x-direction

Table 6 provides the final optimization result for both rounds of Genetic Algorithm compared to the original shape. Based on the improvement achieved in the 1st round GA optimization, the 2nd round GA optimization further improves the fitness value by another 2.8%. According to the final optimization result in Table 6, the total improvement in two rounds of GA optimization is 38.6%; thus the sonic boom signature is significantly minimized. The strength of shock wave is reduced by nearly 40%, which is very significant in reducing the sonic boom near the ground. These results demonstrate that CFD can be accurately and effectively employed for shape optimization of a supersonic airplane to minimize its boom signature.

Table 6: Optimization result from Second round of Genetic Algorithm optimization

	Original SEEB-ALR	1st Round of GA Best shape	2nd Round of GA Best shape
$Max\|P - Pinf\|$	892Pa	572Pa	548Pa
$Max\left\|\frac{\Delta P}{P}\right\|$	0.008803	0.005645	0.005408
Improvement	-	35.8%	38.6%

VI. Sonic Boom Signature Propagation with sBOOM

The most important consequence of supersonic flight and the generated sonic booms is the effect of near field pressure disturbance near the ground. Its footprint near the ground can affect the peoples' health as well other structures such as buildings due to large pressures generated by the boom. The sBOOM program, developed at NASA Langley Research Center can be used to study the propagation of sonic boom in the atmosphere all the way to the ground. It takes the near field pressure data and propagates it through the atmosphere to a desired distance all the way to the ground. The near field solution is propagated by sBOOM using an augmented Burgers equation,

which includes terms for absorption, molecular relaxation, atmospheric stratification and spreading in the classical Burgers' equation [2]. This allows the program to account for the complex interactions that take place as the pressure waveform moves through the atmosphere. Due to the very small scales of the SEEB-ALR and Delta Wing wind tunnels models, they can not be directly used to study propagation through the atmosphere since the resultant pressure from these models felt at the ground level from a cruise altitude of say 45,000 ft would be negligible. Therefore the wind tunnel models are scaled to the commercial aircraft size for boom propagation. Wind tunnel to full scale is handled internally in sBOOM where the propagation is first computed for the smaller wind tunnel model and the ray tubes are then scaled-up to represent data for the "actual" full size body.

VII. Sonic Boom Propagation Results

The results of sonic boom propagation from a height of 45,000 to several heights above the ground are presented for the original SEEB-ALR and optimized shape.

A. SEEB-ALR

The near field ΔP/P produced by the ANSYS simulation shown in Figure 7 was used as the input pressure disturbance from wind tunnel model in the sBOOM program to simulate the pressure signatures at several altitudes between the 45,000 ft cruise altitude and the ground. The signal was propagated from 45,000 ft to each altitude for a SEEB-ALR model scaled to a body length of 202 ft. The results of the propagation are shown in Figure 21. The results of boom signature from the optimized shape were also propagated and are shown in Figure 22.

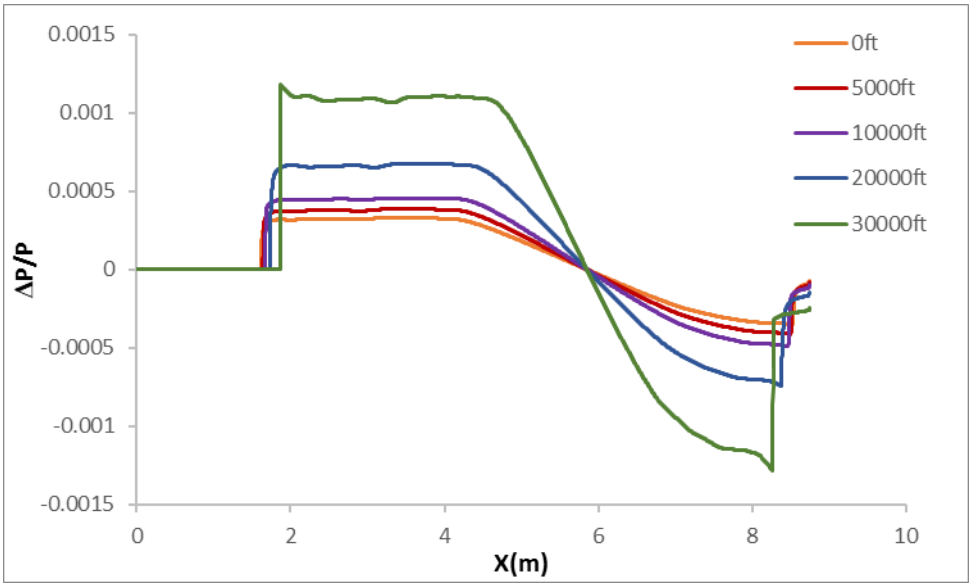

Fig. 21 Pressure signatures propagated from 45K feet for scaled SEEB-ALR model at various altitudes above the ground

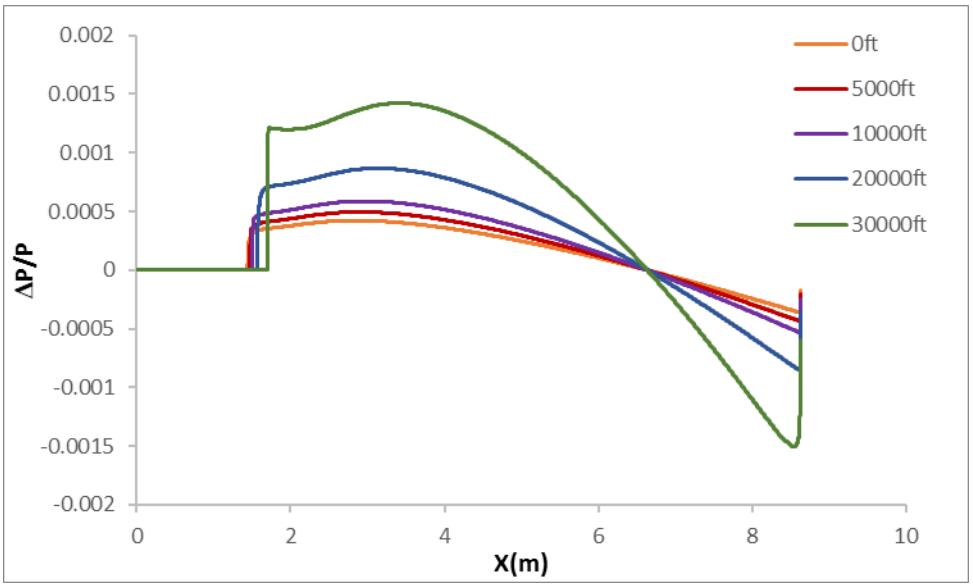

Fig. 22 Pressure signatures propagated from 45K feet for scaled optimized SEEB-ALR model at various altitudes above the ground

B. 69 Degree Delta Wing-Body

The ΔP/P data produced by the Delta Wing simulation in Figure 9 was used as the input wind tunnel data to propagate scaled Delta Wing pressure signatures in sBOOM. The resulting propagation signatures are shown in Figure 23. Both the near field simulation and the scaled propagation signatures show an interesting double N-wave shape for the more complex Delta Wing body configuration. The propagated signature does appear to smooth out the small disturbances visible in the near field data as the signal propagates further towards the ground. Optimization of the boom signature from Delta Wing is currently underway; the boom propagation will be considered once the optimized results become available.

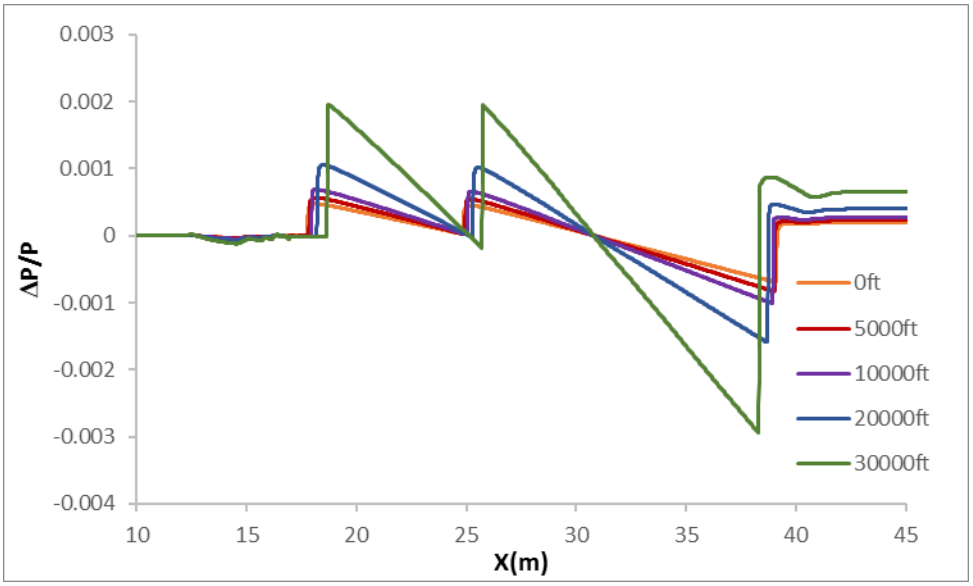

Fig. 23 Pressure signatures propagated from 45K feet for scaled optimized Delta Wing-Body model at various altitudes above the ground

VIII. Conclusions

Simulations of the SEEB-ALR and 69 Degree Delta Wing-Body have been successfully completed and validated. The predicted pressure disturbances in the near field are in excellent agreement with the experimental data. Shape optimized SEEB-ALR body shows a signification reduction in peaks of sonic boom pressure of original SEEB-ALR body. S-Boom was successfully use in comuting the propagation of sonic boom through the atmosphere all the way to the ground.

IX. Acknowledgements

The authors are very grateful to DR. Sivaram Rallabandi of NASA Langley Research Center for providing the s-Boom code.

References

[1]"1st AIAA Sonic Boom Prediction Workshop." http://lbpw.larc.nasa.gov/ [retrieved October 2015]

[2]Rallabhandi, S.K. "Advanced Sonic Boom Prediction Using the Augmented Burgers Equation." Journal of Aircraft (2011): 1245-1253.

[3]Morgenstern, J., Norstrud, N., Sokhey, J., Martens, S. and Alonso, J. J., "Advanced Concept Studies for Supersonic Commercial Transports Entering Service in the 2018 to 2020 Period," Annu. Rev. Fluid Mech., Vol. 44, 2012, pp. 505-526.

[4]Goldberg, D. E., Genetic Algorithms in Search, Optimization, and Machine Learning: Addison-Wesley, 1989.

[5]Morgan, B., "Gairfoils: Finding High-Lift Joukowski Airfoils with a Genetic Algorithm," Technical Report, Dept. of Mechanical Engineering, Washington University in St. Louis, 2007.

[6]Deb, K., "Single and Multi-Objective Optimization Using Evolutionary Computation," Proceedings of the 6th International Conference on Hydro-informatics, Singapore, 2004.

[7]Srinivas, N., and Deb, K., "Multi-objective Optimization Using Non-dominated Sorting in Genetic Algorithms," Evolutionary Computation, Vol. 2, No. 3, 1994, pp. 221-248.

[8]Konak, A., Coit, D. W., and Smith, A. E., "Multi-objective Optimization Using Genetic Algorithms: A Tutorial," Reliability Engineering & System Safety, Vol. 91, No. 9, 2006, pp. 992-1007.

[9]Zaman, M., and Chowdhury, S., "Modified Bezier Curves with Shape-Preserving Characteristics Using Differential Evolution Optimization Algorithm," Advances in Numerical Analysis, 2013.